Articles

Nucleic Acid Binding of the RTN1-C C-Terminal Region: Toward the Functional Role of a Reticulon Protein[†]

Sonia Melino,*,‡ Ridvan Nepravishta,‡ Alessia Bellomaria,‡ Stefania Di Marco,§ and Maurizio Paci‡

Department of Sciences and Chemical Technologies, University of Rome "Tor Vergata", Rome, Italy, and Istituto di Ricerche di Biologia Molecolare P. Angeletti, Pomezia, Rome, Italy

ABSTRACT: RTN1-C protein is a membrane protein localized in the ER and expressed in the nervous system. Its biological role is still unclear, although interactions of the N-terminal region of RTN1-C with proteins involved in vesicle trafficking have been observed, but the role of the C-terminal region of this family protein remains to be investigated. By a homology analysis of the amino acid sequence, we identified in the C-terminal region of RTN1-C a unique consensus sequence characteristic of H4 histone protein. Thus, a 23-mer peptide (RTN1-C$_{CT}$) corresponding to residues 186−208 of RTN1-C was synthesized, and its conformation and its interaction with nucleic acids were investigated. Here we demonstrate the strong ability of RTN1-C$_{CT}$ peptide to bind and condense the nucleic acids using electrophoretic and spectroscopic techniques. To determine if the binding of RTN1-C to nucleic acids could be regulated in vivo by an acetylation−deacetylation mechanism, as for the histone proteins, we studied the interaction of RTN1-C with one zinc-dependent histone deacetylase (HDAC) enzyme, HDAC8, with fluorescence and kinetic techniques using an acetylated form of RTN1-C$_{CT}$. The results reported here allow us to propose that the nucleic acid binding property of RTN1-C may have an important role in the biological function of this protein, the function of which could be regulated by an acetylation−deacetylation mechanism.

Reticulons (RTN)[1] and Nogo proteins make up a family of ER membrane proteins preferentially expressed in the nervous system. Four RTN paralogues (RTN1−3 and RTN4/Nogo) sharing a highly conserved C-terminal region have been identified (*1*). This C-terminal region contains a characteristic reticulon homology domain (RHD) of ∼200 residues. The RHD comprises a variable N-terminal region that is also markedly different in size, with two putative transmembrane regions with a 66-residue hydrophilic loop between them, and a short C-terminal tail (*1*). The conservation of the RHD has already been shown to confer common functions upon RTNs, such as their localization to the

appropriate membranes and mediation of protein interactions. Three splice variants are produced by the *rtn1* gene (RTN1-A, -B, and -C) with a common C-terminal domain (*2*). RTNs were originally classified as markers of neuroendocrine differentiation (*3*), and RTN1-A and -C have been proposed to be molecular markers for the diagnosis of amyotrophic lateral sclerosis (ALS) and peripheral neuropathies in which changes in their expression levels have been observed (*4*). The functions of RTNs are still poorly understood, although their participation has been demonstrated in many biological processes, such as axonal regeneration (*5*), cell death (*6*), and formation of the viral replication complex (*7*). Recently, it has been shown that reticulons interact with a variety of proteins such as antiapoptotic proteins (Bcl-2 and Bcl-xL) (*8*), Golgi glucosylceramide synthase (*9*), soluble *N*-ethylmaleimide-sensitive factor attachment protein receptor (SNARE) proteins (*10*), and BACE1 (*11*), suggesting the involvement of reticulons in different cellular functions from apoptosis induction to membrane vesicle trafficking and APP processing. Moreover, it has been also demonstrated, by in vitro and in vivo immunoprecipitation experiments, that RTN1 is able to interact with the microtubule-interacting and trafficking domain of spastin (*12*), which is a versatile protein involved in microtubule dynamics (*13*) and important for the pathogenesis of the hereditary spastic paraplegia (HSP) (*14*). The N-terminal region of RTN1-C is characterized by

[1] Abbreviations: RTN, reticulons; ER, endoplasmic reticulum; HDAC, histone deacetylase; HAT, histone acetyltransferase; RP-HPLC, reverse phase high-performance liquid chromatography; RHD, reticulon homology domain; SNARE, soluble *N*-ethylmaleimide-sensitive factor attachment protein receptor; APP, amyloid precursor protein; TFE, 2,2,2-trifluoroethanol; T_m, melting temperature; Eth Br, ethidium bromide; FID, fluorescent intercalator displacement; TAcRTN1-C$_{CT}$, acetylated RTN1-C$_{CT}$ peptide; AMC, 7-aminocoumarin; NE, nuclear envelope.

the presence of a unique sequence of amino acid residues 1−20, which has been found to bind SNARE proteins, that are localized on donor vesicles and target organelles and are essential for docking and fusion of the membranes (*15*).

Although reticulons play a role in membrane trafficking, the function of RTN1-C remains elusive, especially the function of the C-terminal region. In this paper, we report the results of a careful analysis of the amino acid sequence of RTN1-C protein and synthesize a peptide corresponding to C-terminal residues 186−208 for the performance of structural and functional studies to elucidate the role of this potential cytosolic region. The primary structure of this region revealed the presence of a highly basic sequence followed by a H4 histone consensus motif. On the basis of the homology analysis, we decided to investigate whether the H4 consensus sequence and the extended basic sequence are involved in DNA binding. A functional study was performed, and the interaction with nucleic acids and a histone deacetylase enzyme was analyzed. Here we show by a shift retardation assay, circular dichroism, and fluorescence spectroscopy that the C-terminal RTN1-C fragment is a possible nucleic acid-binding region of RTN1-C protein. Recently, we have observed that RTN1-C protein expressed in the SH-SY5Y$^{\text{RTN-1C}}$ human neuroblastoma cell line was acetylated (M. Piacentini et al., manuscript in preparation), demonstrating that the function of RTN1-C protein can be regulated in vivo by this posttranslational modification. To determine if the interaction of this protein with nucleic acids could be regulated in vivo by an acetylation−deacetylation mechanism, in which the HDAC (*16*) family enzyme is involved, we investigated the possible interaction of a zinc-dependent HDAC, HDAC8, enzyme with the C-terminal region of RTN1-C.

EXPERIMENTAL PROCEDURES

Peptide Synthesis. Synthetic peptides were purchased from Peptide Specialty Laboratories GmBH and from Spectra 2000 (Rome, Italy). Analysis of the synthetic peptides by reverse phase high-performance chromatography (RP-HPLC) and mass spectrometry revealed a purity of >98%. The two peptides had the following sequences: 32-mer RTN1-C$_{\text{NT(1−32)}}$, NH$_2$-MQATADSTKMDCVWSNWKSQAIDLLY-WRDIKQ-CONH$_2$ (*m/z* 3837.0 ± 0.5); 23-mer RTN1-C$_{\text{CT}}$, NH$_2$-RTHINTVVAKIQAKIPGAKRHAE-CONH$_2$ (*m/z* 2535.69 ± 0.5).

Circular Dichroism. CD measurements were performed using a Jasco 600 spectropolarimeter (Jasco, Tokyo, Japan) calibrated with camphorsulfonic acid. CD spectra were obtained between 200 and 250 nm using a path length of 0.1 cm and between 600 and 300 nm using a path length of 1 cm, a time constant of 1.0 s, a bandwidth of 2 nm, and a scan rate of 2 nm/min with a sensitivity of 20 or 50 mdeg. The average was corrected by four scans of the solvent; 0.1−1 cm path length quartz cells sealed and controlled thermostatically were used for the far- and near-UV CD measurements, respectively. The circular dichroism measurements were performed with 50 and 150 μM peptide and at different concentrations of 2,2,2-trifluoroethanol (TFE) at room temperature (23 °C).

DNA and RNA Binding. Plasmid DNA (pQE30-rhdA) was isolated from *Escherichia coli* using a Plasmid Mini Kit

(Sigma-Aldrich, Milan, Italy). The gel retardation assay was performed mixing the plasmid DNA (0.5 μg) with increasing amounts of RTN1-C$_{\text{CT}}$ peptide (from 0 to 5 μg) in 20 mM Tris (pH 7.5). After incubation for 2 min at room temperature, the samples were electrophoresed on a 0.8% agarose gel in TAE buffer (40 mM Tris-acetate and 1 mM EDTA) for 80 min at 60 V and stained with ethidium bromide. For the competitive interaction studies, 4 μg of pDNA was incubated with RTN1-C$_{\text{CT}}$ in a peptide/pDNA ratio of 10/1 (w/w) for 10 min at room temperature. *Sma*I restriction enzyme (15 units) (Fermentas, M-Medical, Milan, Italy) and Tango buffer (Fermentas, M-Medical) were added to the solution, and a time course of the digestion was performed at 30 °C (0, 15, 30, and 60 min). The reactions were terminated by addition of 2 μL of 6× gel loading buffer (5% glycerol, 0.125% bromophenol blue, and 25 mM EDTA) and the mixtures kept at −20 °C. The samples were electrophoresed on a 1% agarose gel for 60 min at 70 V and stained with ethidium bromide (Eth Br).

RNA was extracted by *E. coli* cells using the RNAspin Mini Kit (GE Healthcare), and the gel retardation assay was performed by mixing rRNA (1.0 μg) in the presence of increasing amounts of RTN1-C$_{\text{CT}}$ or RTN1-C$_{\text{NT(1−32)}}$ peptide (from 0 to 10 μg) in 20 mM Tris-HCl buffer (pH 7.5). The samples were electrophoresed on a 2% agarose gel at 60 V and stained with ethidium bromide. To the solution with RTN1-C$_{\text{NT(1−32)}}$ was added 1 mM DTT for inhibition of dimer formation.

Fluorescent Intercalator Displacement Assay. The concentration of the pDNA stock solution was determined spectroscopically, and 3 μg of pDNA or DNA ladder (Sigma-Aldrich) was added with 900 μL of Eth Br (1.5 μg/mL) in 10 mM Hepes buffer (pH 7.0). Fluorescence studies were carried out with a Perkin-Elmer LS luminescence spectrometer using a λ_{ex} of 523 nm, a λ_{em} of 535−600 nm, a path length of 1 cm, a 1 mL quartz cuvette, and a slit width of 5 nm. A plot of the fluorescence changes versus the number of equivalents of peptide provides a titration curve from which the stoichiometry may be determined (*17, 18*). ΔF was plotted versus the number of molar equivalents of peptide, and the following equations were used to generate a Scatchard plot from which binding constants could be determined:

$$(\Delta F_{\text{x}}/\Delta F_{\text{sat}})/X = \text{fraction of DNA−peptide complex} \quad (1)$$

$$[1 - (\Delta F_{\text{x}}/\Delta F_{\text{sat}})/X] = \text{fraction of peptide free} \quad (2)$$

$$[\text{DNA}]_{\text{T}}(X - \Delta F_{\text{x}}/\Delta F_{\text{sat}}) = [\text{free peptide}] \quad (3)$$

where [free peptide] is the concentration of free peptide, [DNA]$_{\text{T}}$ is the total concentration of oligo dsDNA (ds[CG]$_5$ and ds[GT]$_5$), X corresponds to the number of molar equivalents of agent versus DNA, ΔF_{x} is the change in fluorescence, and ΔF_{sat} is the change in fluorescence at the point where DNA is saturated with peptide.

Thermal Denaturation Studies. Thermal denaturation experiments were performed on a Perkin-Elmer Lambda Bio20 double-beam spectrophotometer using a 1 cm path length sealed quartz cuvette incorporating the temperature sensor closed with a Teflon cap. The temperature was controlled with a programmable Peltier temperature-controlled cell holder. The absorbance of each DNA sample was ∼1.5 μM, in 10 mM Hepes buffer (pH 7.0). Oligonucleotide

annealing was performed before thermal analysis by heating the sample at 95 °C followed by slow cooling to the starting temperature. Melting profiles were acquired by heating samples from 7 to 85 °C at a rate of 1 °C/min and measuring the absorbance corresponding to the maximum around 260 nm. Condensation of water vapor in the cuvette holding chamber at low temperature was prevented by flushing N_2 gas. The melting temperature (T_m) was estimated from the maximum of the first-derivative curve of absorbance versus temperature.

Preparation of Acetylated RTN1-C_{CT}. Chemical acetylation of RTN1-C_{CT} peptide was conducted using a modified method of Cary et al. (*19*). Briefly, at 2 mg/mL peptide, in 100 mM ammonium bicarbonate (pH 10), acetic anhydride was added using a 100:1 (c/c) molar ratio of acetic anhydride to lysine residues and the solution was kept on ice for 10 min, and the reaction was stopped by freezing the mixture after lyophilization. During the reaction, a rapidly decreasing pH was observed. The acetylated peptide (TAcRTN1-C_{CT}) was purified from the reaction mixture by RP-HPLC using a C18 column and then checked by acid−urea gel electrophoresis. The acetylation of the ε-amino group of the lysine side chains was observed by high-resolution one-dimensional ^{1}H NMR spectra recorded at 25 °C using a Bruker 400 MHz NMR spectrometer equipped with a z-gradient as previously described by Cary et al. (*19*). The samples were then analyzed by LC−MS via ESI mass spectroscopy (by Colosseum Combinatorial Chemistry Centre Tecnology, C4T, Rome, Italy) using a single-quadrupole spectrometer (Thermo Surveyor MSQ, Waltham, MA) with positive modality acquisition from *m/z* 200 to 2000. The instrument was calibrated with a solution standard, Ultramark 1621.

Cationic Electrophoresis. Acetylated RTN1-C_{CT} peptides were analyzed on a 20% acid−urea polyacrylamide running gel, containing 5.8 M urea and 5% acetic acid (gel dimensions of 10 cm × 10 cm × 0.75 mm) and using a 7.5% stacking gel, with 5.3 M urea and 5% acetic acid. The gels were prerun at 200 V for ∼1.30 h using 5% acetic acid. After prerunning had been carried out, the gels were run at 200 V and the methylene green was used as a dye. Gels were stained in 0.1% Amido Black, 40% methanol, and 10% acetic acid and destained in several changes of 10% acetic acid and 1% ethanol.

HDAC8 Protein Expression and Purification. Overexpression of the recombinant HDAC8 protein in *E. coli* and purification were performed as described by Vannini et al. (*20*).

HDAC Assay. Fluorescence activity assays of HDAC8 protein were performed using the Fluor de-Lys, fluorogenic deacetylase substrate, (acetyl)-Arg-His-Lys(ε-acetyl)-Lys-coumarin, according to the manufacturer's instructions (BIOMOL International LP, Plymouth Meeting, PA). Briefly, 0.12−1.12 μM HDAC8 recombinant protein, in 50 mM Tris-HCl (pH 8.0), 137 mM NaCl, 2.7 mM KCl, and 1 mM $MgCl_2$, was used, and the reaction was started adding 5 μL of substrate solution (final concentration of 100 μM) to 45 μL of sample solution followed by incubation for 60 min at 37 °C. The reaction was stopped by addition of 50 μL of trypsin/TSA stop solution [10 mg/mL trypsin from porcine pancreas (Sigma-Aldrich) in 100 mM ammonium bicarbonate (pH 8.0) and 2 μM TSA]. The release of AMC was monitored by measuring the fluorescence at 460 nm (λ_{ex} = 360 nm) after incubation for 20 min at 30 °C. The AMC signals were recorded against a blank with buffer and substrate but without the enzyme. We observed the inhibition effects of the peptides after preincubation of the enzyme for 15 min in their presence, at room temperature, before the addition of the substrate. All experiments were conducted in triplicate.

Fluorescence Interaction Studies. The interaction of RTN1-C_{CT} and TAcRTN1-C_{CT} peptides with 1.5 μM HDAC8 was monitored by quenching of the emission band of HDAC8 excited at 280 nm using λ_{ex} and λ_{em} slits of 5 nm in 25 mM Tris-HCl (pH 8.0), 0.10 M NaCl, and 2 mM KCl at 27 °C.

Binding constants were determined using the same equations reported above, as described by Boger et al. (*18*). ΔF_x was the observed fluorescence change after addition of peptide; ΔF_{sat} was the change in fluorescence at the point where the enzyme (E) was saturated with peptide. Fluorescence was measured at the chemical equilibrium at the earliest 2 min after addition of inhibitor. The results were plotted using GraphPad Prism version 4.0 for Windows (GraphPad Software, San Diego, CA).

RESULTS

H4 Consensus Sequence Identification. Functional characterization of a protein is often improved by the identification of its interaction partners and by use of programs to screen sequence databases for the prediction of functional sites. A careful analysis of the amino acid sequence of RTN1-C protein was performed, and a consensus sequence, which was characteristic of H4 histone (PS000047 HISTONE_H4), was found in the C-terminal region of RTN1-C using PROSITE (http://expasy.org/tools/scanprosite/). H4 histone is a protein that has remained almost invariant for more then 2 billion years of evolution (*21*), and the consensus sequence used as a signature pattern corresponds to the GA**K**RH pentapeptide that has been found in positions 14−18 of all H4 histone sequences. InterProScan (*22*) (http://npsa-pbil.ibcp.fr/gcg-bin/pattern_pattinprot.pl) was used to identify protein sequences, in the UniProt sequence database, that have the characteristic pattern G-A-K-R-H. From this analysis, the characteristic pattern was found to be present, with 100% similarity, only in histone H4, in the reticulon 1 and in catalase A proteins (SwissProt entry CATA_EMENI). Figure 1A shows the alignment between the amino acid sequences of the C-terminal domain of human RTN1-C and the N-terminal region of H4. Notably, residues H18 and K16, which are present in the recognition pattern of H4, are also implicated in DNA binding, and proper chromatin folding requires the presence of residues 14−19 (*23, 24*). K16 is intimately involved in regulating DNA topology (*25*); in fact, it is often acetylated and is involved in the regulation system of gene expression (*26*). Recent structural studies have shown that acetylation of K16 disrupts the formation of compacted chromatin by inhibiting the interfiber interaction (*27*). The acetylation of ε-aminolysine is a reversible posttranslational modification, and the acetylation status of the lysine residues at the N-terminal extension of the histones is controlled by two counteracting enzymes: histone acetyltransferase (HAT) and histone deacetylase (*16, 28*). HDACs, also, participate in the regulation of non-histone proteins and are important in many biological processes, which are modulated during

```
                                                        8       12      16
H4 HUMAN 8-20                                          KGLGK-GGAKRHRK
RTN1-C HUMAN 186-208        RTHINAVVAKIQAKIPGAKRHAE
                                                       *   .*  ***** :
```

```
Q9BQ59_HUMAN            MQATADSTKMDCVWSNWKSQAIDLLYWRDIKQTGIVFGSFLLLLFSLTQFS
Q1LZ76_BOVIN            MQATADSTKMDCVWSNWKSQAIDLLYWRDIKQTGIVFGSFLLLLFSLTQFS
Q7M6W1_MOUSE            MQATADSTKMDCVWSNWKSQAIDLLYWRDIKQTGIVFGSFLLLLFSLTQFS
Q6IM72_CANFA            MQATADFTKMDCVWSNWKSQAIDLLYWRDIKQTGIVFGSFLLLLFSLTQFS
Q5IS59|RTN1_PANTR(586-776)      KQKAIDLLYWRDIKQTGIVFGSFLLLLFSLTQFS
Q16799|RTN1_HUMAN(586-776)      KQKAIDLLYWRDIKQTGIVFGSFLLLLFSLTQFS
Q64548|RTN1_RAT  (587-777)      KQKAIDLLYWRDIKQTGIVFGSFLLLLFSLTQFS
                       ******.********* *.:******************************

Q9BQ59_HUMAN            VVSVVAYLALAALSATISFRIYKSVLQAVQKTDEGHPFKAYLELEITLSQE
Q1LZ76_BOVIN            VVSVVAYLALAALSATISFRIYKSVLQAVQKTDEGHPFKAYLELEITLSQE
Q7M6W1_MOUSE           VVSVVAYLALAALSATISFRIYKSVLQAVQKTDEGHPFKAYLELEITLSQE
Q6IM72_CANFA           VVSVVAYLALAALSATISFRIYKSVLQAVQKTDEGHPFKTYLELEITLSQE
Q5IS59|RTN1_PANTR      VVSVVAYLALAALSATISFRIYKSVLQAVQKTDEGHPFKAYLELEITLSQE
Q16799|RTN1_HUMAN      VVSVVAYLALAALSATISFRIYKSVLQAVQKTDEGHPFKAYLELEITLSQE
Q64548|RTN1_RAT        VVSVVAYLALAALSATISFRIYKSVLQAVQKTDEGHPFKAYLELEITLSQE
                       ***********************************:***********

Q9BQ59_HUMAN           QIQKYTDCLQFYVNSTLKELRRLFLVQDLVDSLKFAVLMWLLTYVGALFNG
Q1LZ76_BOVIN           QIQKYTDCLQFYVNNTLKELRRLFLVQDLVDSLKFAVLMWLLTYVGALFNG
Q7M6W1_MOUSE           QIQKYTDCLQLYVNSTLKELRRLFLVQDLVDSLKFAVLMWLLTYVGALFNG
Q6IM72_CANFA           QIQKYTDCLQFYVNNTLKELRRLFLVQDLVDSLKFAVLMWLLTYVGALFNG
Q5IS59|RTN1_PANTR      QIQKYTDCLQFYVNSTLKELRRLFLVQDLVDSLKFAVLMWLLTYVGALFNG
Q16799|RTN1_HUMAN      QIQKYTDCLQFYVNSTLKELRRLFLVQDLVDSLKFAVLMWLLTYVGALFNG
Q64548|RTN1_RAT        QIQKYTDCLQLYVNSTLKELRRLFLVQDLVDSLKFAVLMWLLTYVGALFNG
                       **********:***.***********************************

Q9BQ59_HUMAN           LTLLLMAVVSMFTLPVVYVKHQAQIDQYLGLVRTHINAVVAKIQAKIPGAK
Q1LZ76_BOVIN           LTLLLMAVVSMFTLPVVYVKHQAQIDQYLGLVRTHINAVVAKIQAKIPGAK
Q7M6W1_MOUSE           LTLLLMAVVSMFTLPVVYVKHQAQVDQYLGLVRTHINTVVAKIQAKIPGAK
Q6IM72_CANFA           LTLLLMAVVSMFTLPVVYVKHQAQIDQYLGLVRTHINTVVAKIQAKIPGAK
Q5IS59|RTN1_PANTR      LTLLLMAVVSMFTLPVVYVKHQAQIDQYLGLVRTHINAVVAKIQAKIPGAK
Q16799|RTN1_HUMAN      LTLLLMAVVSMFTLPVVYVKHQAQIDQYLGLVRTHINAVVAKIQAKIPGAK
Q64548|RTN1_RAT        LTLLLMAVVSMFTLPVVYVKHQAQVDQYLGLVRTHINTVVAKIQAKIPGAK
                       ************************:*************:************

Q9BQ59_HUMAN           RHAE
Q1LZ76_BOVIN           RHTE
Q7M6W1_MOUSE           RHAE
Q6IM72_CANFA           RHAE
Q5IS59|RTN1_PANTR      RHAE
Q16799|RTN1_HUMAN      RHAE
Q64548|RTN1_RAT        RHAE
                       **:*
```

FIGURE 1: Homology of the amino acid sequences of RTN1-C. The top panel shows the overlapping of the amino acid sequences of H4 and RTN1-C proteins. The H4 consensus sequence is highlighted in gray. Multiple alignments of reticulon proteins, which conserve the H4 consensus sequence, are also shown. Multiple alignments were generated using CLUSTALW (*57*).

malignant transformations (*29*). On the basis of this observation, we investigated the ability of the C-terminal region of RTN1-C to bind nucleic acids and to interact with HDAC enzymes. Figure 1B shows multiple alignments of amino acid sequences of all RTN proteins that present the histone consensus sequence.

Structural Analysis of the C-Terminal Region of RTN1-C. Secondary structure predictions for the C-terminal region (residues 179−208) of RTN1-C, performed using GOR-IV and AGADIR (http://npsa-pbil.ibcp.fr/cgi-bin/npsa_automat. pl?page=npsa_gor4.html and http://www.embl-heidelberg.de/ Services/serrano/ agadir/agadir-start.html) (Figure 2A), indicated the possible formation of α-helix in the region from residue 190 to 199. Thus, a RTN1-C$_{CT}$ peptide corresponding to the C-terminal region of RTN1-C from residue 186 to 208, which represents the minimal sequence that includes the region that has propensity to assume helix conformation and the histone H4 consensus sequence, was synthesized and analyzed by circular dichroism. Figure 2B shows CD spectra of RTN1-C$_{CT}$ peptide in a water solution at different percentages of 2,2,2-trifluoroethanol (TFE). The mean resi-

due ellipticity observed was independent of the peptide concentration, indicating that the peptide was essentially monomeric under the experimental conditions that were used. The profile of the ellipticity of the peptide in a water solution (pH 6.1) was characteristic of a peptide which does not have a stable conformation, but an enhancement of the negative ellipticity at 208 and 222 nm ($[\theta]_{222}/[\theta]_{208}$ ratio of ∼0.7), indicating that the formation of a helix conformation was induced by the increase in the TFE concentration. Helix conformation, at 30% (v/v) TFE, was estimated to correspond to 25% of the length of the peptide, using K2d (http://kal-el.ugr.es/k2d/k2d.htlm) (*30*). RTN1-C$_{CT}$ peptide is characterized by the presence of a capping-box motif (**S/TXXD/N**), which has been identified as an initiator and stabilizer of α-helices in peptides and proteins (*31*). Thus, the propensity of the peptide to assume an α-helical conformation in a hydrophobic environment could be explained by the presence of this structural motif. Our results are in agreement with secondary structure predictions of the C-terminal region of RTN1-C and allow us to propose that the C-terminal region of RTN1-C protein, which in the structural model is present
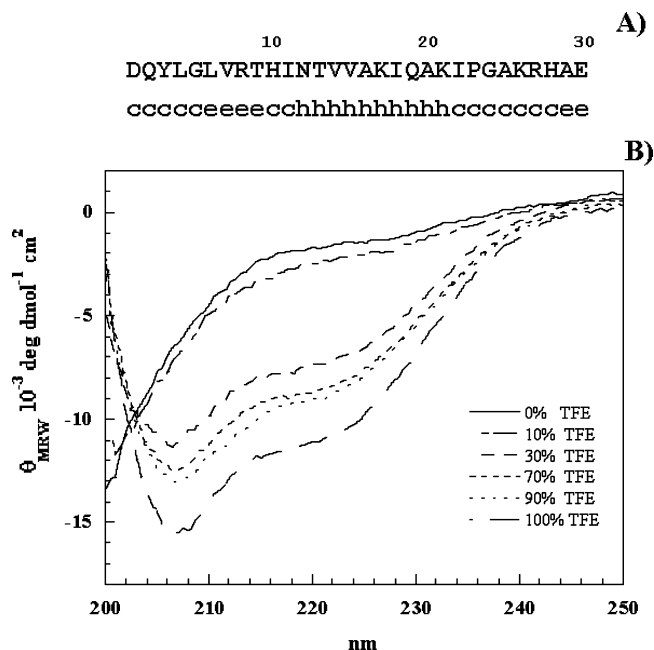
FIGURE 2: Secondary structure of RTN1-C_{CT}. (A) Prediction of the structure of the C-terminal region of RTN1-C, from residue 179 to 208, obtained using GOR-IV (*58*). (B) CD spectra of 50 μM RTN1-C_{CT} peptide as a function of TFE concentration in water (—) and in 10% (- —), 30% (— — —), 70% (---), 90% (•••), and 100% TFE (———).

in the cytoplasm and close to the ER membrane (*32, 33*), may assume in vivo a stable α-helical conformation.

RTN1-C_{CT} Binds both DNA and RNA. The DNA binding ability of RTN1-C_{CT} was evaluated in a gel retardation assay. Peptide was mixed with a fixed amount of plasmid DNA to produce a 0, 1, 2, 3, 5, or 10 peptide:DNA (w/w) ratio, and the complexes were electrophoresed on an agarose gel (Figure 3A). At a peptide:pDNA weight ratio of 2:1, a fraction of pDNA remained at the origin (a_1 band), and this effect was more evident at higher peptide:DNA ratios, showing that the DNA was aggregated by RTN1-C_{CT} peptide. Similar patterns of migration have been observed with other peptides (*34, 35*), which showed a strong ability to bind and aggregate the DNA. On the other hand, RTN1-$C_{NT(1-32)}$ peptide did not change the pDNA electrophoretic mobility (see Figure 1S of the Supporting Information), showing that it did not bind the DNA.

The DNA binding ability of the peptide was also evaluated by competition experiments using *Sma*I restriction enzyme. *Sma*I recognizes two sites inside pQE30-rhdA and normally is able to cleave this plasmid (a band) into two fragments, of ~3900 bp (b band) and 500 bp (not visible in the picture) (Figure 3B). Preincubation of pDNA in the presence of RTN1-C_{CT} peptide induced an evident DNA retardation shift and the nonappearance of the b band. Instead, *Sma*I was able to cleave the pDNA in the presence of RTN1-$C_{NT(1-32)}$ peptide, which did not bind pDNA with high efficiency, and therefore, the formation of the b band at 3900 bp was observed (Figure 3B, lanes 6–8). These results show that RTN1-C_{CT} peptide has an intrinsic DNA binding ability and can inhibit the interaction of DNA with other proteins. The DNA binding ability of the peptide was also analyzed by CD spectroscopy, and a significant change in ellipticity after addition of pDNA to RTN1-C_{CT} peptide solution was observed (Figure 4). The spectrum of the mixture was
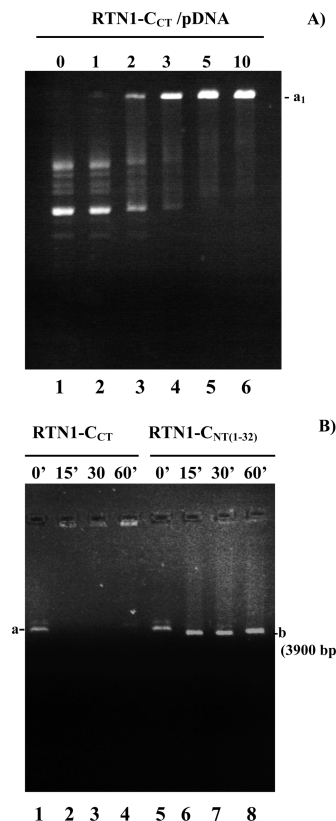

FIGURE 3: pDNA binding of RTN1-C_{CT}. (A) Gel retardation shift assay at different peptide:pDNA weight ratios using 0.5 μg of pQE30-rhda: 0 (lane 1), 1 (lane 2), 2 (lane 3), 3 (lane 4), 5 (lane 5), and 10 (lane 6). In a 0.8% agarose gel at 60 V. The a_1 band is due to the retardation shift effect of RTN1-C_{CT} on the pDNA. (B) Agarose gel electrophoresis (1% agarose) of 0.5 μg of pQE30-rhdA after cleavage with *Sma*I (0.5 unit/μg) after 0 (lane 1), 15 (lane 2), 30 (lane 3), and 60 min (lane 4) at 30 °C in the presence of RTN1-C_{CT} peptide, in a 10:1 (w/w) peptide:pDNA ratio, or in the presence of RTN1-$C_{NT(1-32)}$ after 0 (lane 5), 15 (lane 6), 30 (lane 7), and 60 min (lane 8). The a band corresponds to the linear form of pDNA (4300 bp), while the b band corresponds to the *Sma*I digest fragment of ~3900 bp.
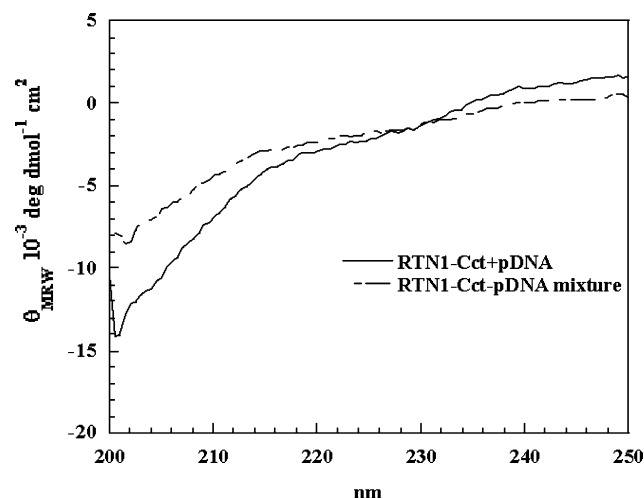

FIGURE 4: Interaction between RTN1-C_{CT} and DNA induces conformational changes of the molecules. CD spectra of a mixture of 50 μM RTN1-C_{CT} and 1 μg of pDNA (- —-) and a sum of the spectra of the single components (—).

different from the sum of the spectra of the two components, indicating an interaction between the two macromolecules.
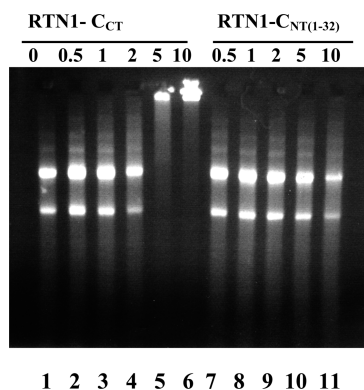
FIGURE 5: RNA binding of RTN1-C$_{CT}$. Gel retardation shift assay of 1 μg of bacterial RNA at 0, 0.5, 1, 2, 5, and 10 RTN1-C$_{CT}$:RNA weight ratios (lanes 1−6, respectively) and at 0.5, 1, 2, 5, and 10 RTN1-C$_{NT(1−32)}$:RNA weight ratios (lanes 7−11, respectively). In a 2% agarose gel at 60 V.

To analyze the possible interaction of RTN1-C$_{CT}$ peptide with other nucleic acids, a RNA retardation gel shift assay was performed (Figure 5). RNA was purified from bacteria as described in Experimental Procedures. A retardation shift of RNA was observed at a RNA:RTN1-C$_{CT}$ ratio of 1:5 and 1:10 (w/w), indicating an interaction between RTN1-C$_{CT}$ and RNA. On the other hand, no mobility shift of RNA in the presence of the same concentration of RTN1-C$_{NT(1−32)}$ peptide was observed. All these data clearly highlight the property of the C-terminal fragment of RTN1-C to bind the nucleic acids in vitro.

DNA Condensation and DNA Binding Sequence Preference of RTN1-C$_{CT}$. Artificial or naturally derived cationic peptides have been widely studied for their DNA condensation ability and used as part of synthetic gene delivery systems exploiting their intrinsic biological activity for enhancing the gene delivery process. We investigated the ability of RTN1-C$_{CT}$ peptide to condense the DNA to improve our understanding of the physiological role of RTN1-C protein. Displacement of Eth Br from DNA provides a direct method of measuring the binding affinity of compounds that lack a chromophore. The fluorescence of free Eth Br in solution was strongly quenched by aqueous solvent and was weak (Figure 6A), and when DNA was added to the solution, a significant fluorescence enhancement due to DNA binding was observed, as reported previously (*36*) (Figure 6A). A time-dependent fluorescence decrease was observed when RTN1-C$_{CT}$ peptide was added to the DNA/Eth Br mixture (Figure 6C). This observed decrease was explained as being due to the existence of an equilibrium of the Eth Br between the intercalated sites and free forms in solution. Thus, the loss of molecular flexibility in the double-stranded structure of DNA through condensation results in a shift in the binding of Eth Br into the solution phase, with the resultant decrease in fluorescence. No fluorescence decay was observed in the presence of RTN1-C$_{NT(1−32)}$ (Figure 6B) during the same time, indicating that the pDNA condensation was a peculiarity of the C-terminal fragment of RTN1-C. Moreover, the preincubation of pDNA with the RTN1-C$_{CT}$ peptide inhibited Eth Br−DNA binding, as shown in Figure 6D. The same experiment was also performed using a DNA ladder, and in this case, a more rapid fluorescence decrease was induced by the addition of RTN1-C$_{CT}$ (Figure 7B).
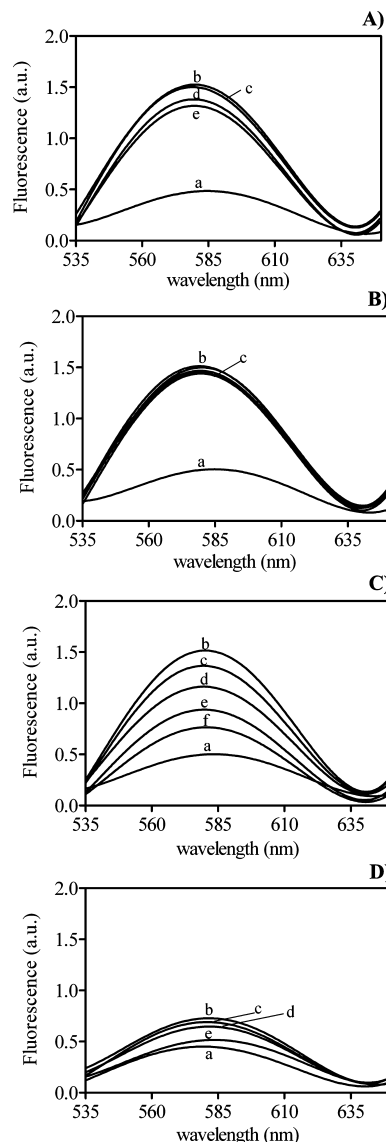

FIGURE 6: DNA condensation as measured by an ethidium bromide exclusion assay. (A) Fluorescence spectra of Eth Br (1.5 μg/mL) alone (a), in 1 mL of 10 mM Hepes (pH 7.0) and bound to 3 μg of pDNA (b), and after 3 (c), 24 (d), and 48 h (e); (B) in the presence of RTN1-C$_{NT(1−32)}$ (c) and after the same amount of time; (C) in the presence of RTN1-C$_{CT}$ (c) and after 3 (d), 24 (e), and 48 h (f) (a decrease in Eth Br fluorescence was observed when the incubation time was increased from 0 to 48 h). (D) Fluorescence spectra of Eth Br after addition of the RTN1-C$_{CT}$−pDNA complex (b) and after 3 (c), 24 (d), and 48 h (e). All incubations were conducted at room temperature with a 1:10 peptide:DNA mass ratio.

To further evaluate the sequence selectivity of RTN1-C$_{CT}$, the interaction experiments were performed using DNA oligomers with ds[CG], ds[GT], and ds[AG] duplex sequences, and melting curves at different peptide concentrations were achieved. In Table 1, the T_m values of the oligonucleotides in the absence and presence of the peptide are reported, and a change in the T_m was observed to be concentration-dependent (see Figure 8A,B). The presence of A·T base pairs promoted the binding of RTN1-C$_{CT}$ to the double strand, as observed from variation of T_m at a 1:10 dsDNA:peptide molar ratio.

The Eth Br displacement assay was performed at different concentrations of RTN1-C$_{CT}$ using ds[CG] and ds[GT] for the calculation of the binding constants (*17, 18*). ΔF values
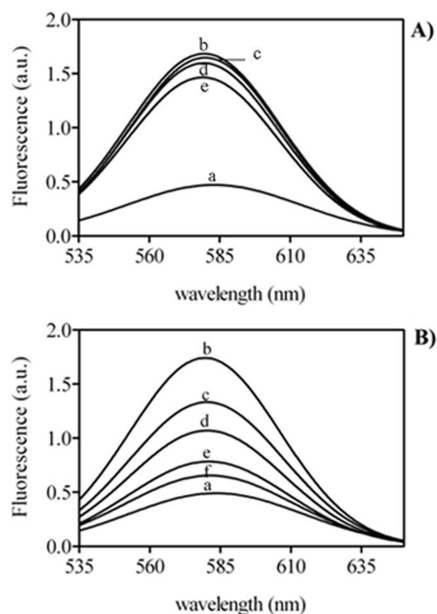
FIGURE 7: DNA ladder condensation by RTN1-C_{CT} as measured by an ethidium bromide exclusion assay. Fluorescence spectrum of Eth Br (1.5 μg/mL) alone (a) and bound to 3 μg of DNA ladder (b), in 10 mM Hepes (pH 7.0), after incubation for ϕ (c), 3 h (d), 24 h (e), and 48 h (f) at room temperature, in the presence of RTN1-$C_{NT(1-32)}$ A) and in the presence of RTN1-C_{CT} (B) using a 10:1 peptide/DNA mass ratio.

Table 1: Transition Temperatures ($T_m \pm 0.5$ °C) of Thermal Denaturation of Different Double-Stranded DNAs in 10 mM Hepes (pH 7.4)

	T_m (°C)		
	0:1 RTN1-1C_{CT}:DNA	1:10 RTN1-1C_{CT}:DNA	ΔT_m (°C)
ds[CG]	47.9	56.6	8.7
ds[GT]	27.2	40.4	13.2
ds[AG]	15.3	27.5	12.2

were plotted versus the number of molar equivalents of peptide, and a Scatchard plot was generated showing that RTN1-C_{CT} was able to bind ds[CG] and ds[GT] with binding constants of 4.7 $\pm$ 1.19 and 1.06 $\pm$ 0.15 μM, respectively (Figure 9A,B). Although RTN1-C_{CT} was able to bind both the double strands, the affinity for DNA was enhanced with the A·T base pair content in the double strand.

Acetylation of RTN1-C_{CT} Peptide. A fully acetylated form of RTN1-C_{CT} (TAcRTN1-C_{CT}) was produced by a chemical acetylation reaction (*19*) of RTN1-C_{CT} peptide. After lyophilization, the acetylated peptide was purified from the reaction mixture by RP-HPLC. This chemical acetylation leads to the acetylation of the N-terminus and of all ε-NH$_2$ groups of Lys residues, so we observed a large difference in the retention times for the two forms. In particular, RTN1-C_{CT} and TAcRTN1-C_{CT} peptides were eluted after 31.46 and 40.57 min, respectively, using the same linear gradient (Figure 2SA of the Supporting Information). The purity and different electrophoretic mobility due to the presence of acetyl groups were also checked by acid−urea gel electrophoresis (Figure 2SB). The molecular mass of the fully acetylated form was *m/z* 2704.14 $\pm$ 0.5, corresponding to the peptide with four acetyl groups (see Figure 3S of the Supporting Information). Acetylation of the ε-amino group of the lysine residues was manifested in the NMR spectrum, as also described by Cary et al. (*19*), by the diagnostic
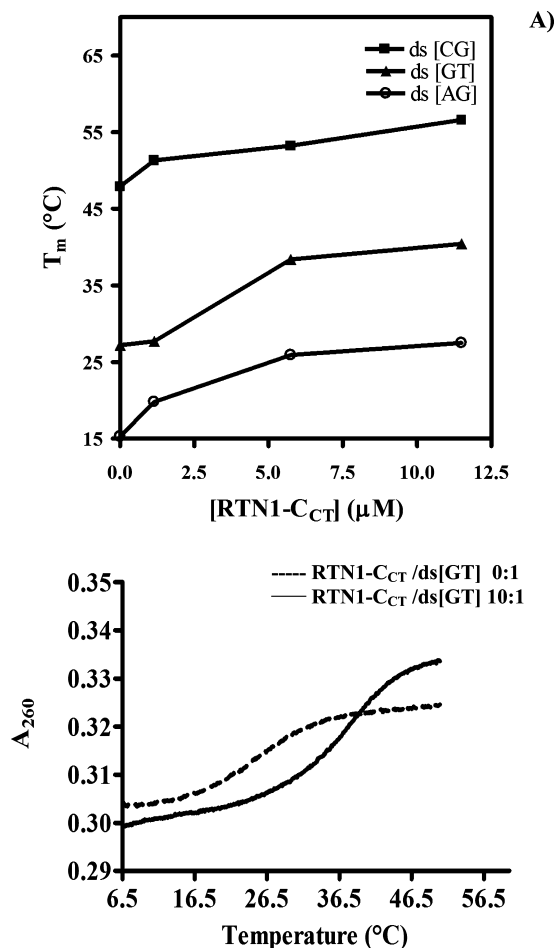

FIGURE 8: (A) Transition temperatures of thermal denaturation of dsDNA and its complex with RTN1-C_{CT} at different peptide:DNA mass ratios: (■) ds[CG], (▲) ds[GT], and (○) ds[AG]. The DNA concentration was kept constant at 1.5 μM, and the peptide: DNA molar ratio was 1:1, 5:1, or 10:1. (B) Thermal denaturation of the RTN1-C_{CT}−ds[GT] complex. The DNA concentration was kept constant at 1.5 μM, and the peptide:DNA molar ratio was varied from 0 (---) to 10 (—).

appearance of a strong CH$_3$ peak of the acetyl group at 1.8 ppm and by the shift of the lysine ε-CH$_2$ peak from 2.91 to 3.07 ppm. Acetylation of the α-amino terminus as seen from the peak at 1.97 ppm was also observed (see Figure 4S of the Supporting Information).

No aggregation of both RTN1-C_{CT} and TAcRTN1-C_{CT} peptides was observed by NMR and CD analysis at different concentrations of the peptides, indicating that they were essentially monomers under the experimental conditions employed (data not shown). The secondary structure of the acetylated peptide was evalued by CD measurements, and like RTN1-C_{CT}, the acetylated peptide had a dichroic spectrum which is characteristic of an helix conformation at 30% TFE (see Figure 5S of the Supporting Information), but with less negative values of ellipticity at 208 and 222 nm that are indicative of a weakened propensity to assume an α-helix conformation.

The interaction of TAcRTN1-C_{CT} with pDNA was also investigated, and the acetylation markedly reduced the affinity of the peptide for DNA, as previously observed for the histone H4 peptide by Hong et al. (*37*) (see Figure 6S of the Supporting Information). FID experiments, further, showed that the ability of the peptide to condense DNA,
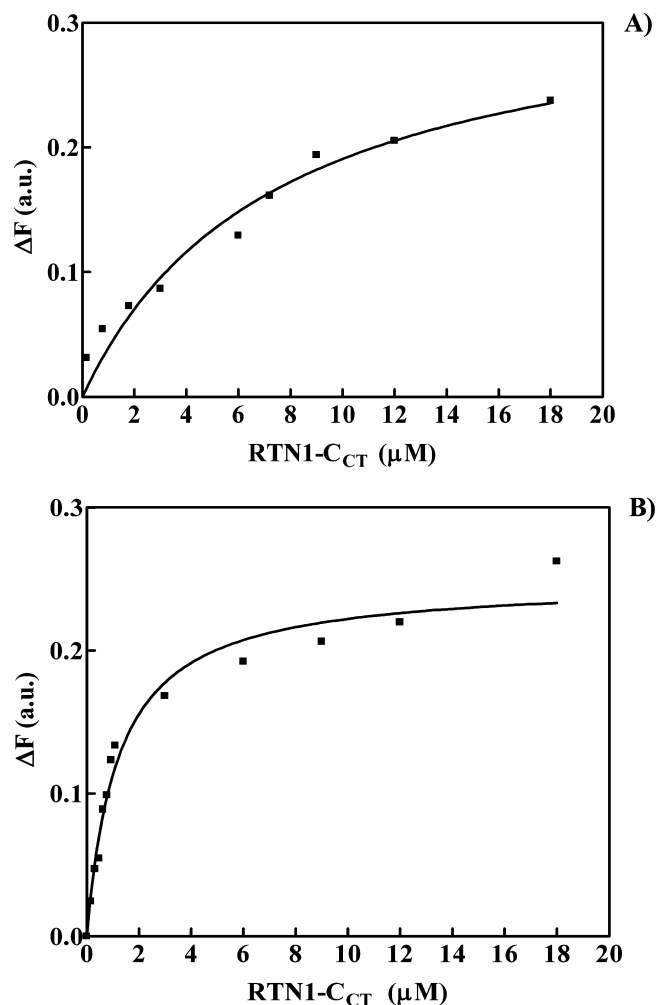
FIGURE 9: Changes in the fluorescence intensity of the ds[DNA]−Eth Br complex upon titration with increasing concentrations of RTN1-C_{CT} peptide (from 0 to 15 equiv): (A) 1.2 μM ds[GC]−Eth Br and (B) 1.2 μM ds[GT]−Eth B complexes. Experiments were conducted in 100 mM Hepes (pH 7.0) at 27 °C, with a λ_{ex} of 523 nm and a λ_{em} from 535 to 650 nm.

under same conditions used for RTN1-C_{CT}, was inhibited by acetylation (see Figure 7S of the Supporting Information). TAcRTN1-C_{CT} was then used to perform interaction and kinetic experiments with the HDAC enzyme, HDAC8.

RTN1-C_{CT} Interacts with Members of the HDAC Enzyme Family. The interaction of RTN1-C_{CT} and TAcRTN1-C_{CT} peptides with HDAC8 was monitored by measuring the fluorescence emitted by the protein. The intrinsic fluorescence of HDAC8 was quenched by the addition of both peptides in a concentration-dependent manner as shown in Figure 10. The binding profiles of *F* versus [peptide] have a hyperbolic shape; this can mean that the protein binds one peptide molecule or more than one with either $F_{complex}$ being linearly related to *n* [$\Delta F = nK[\text{peptide}]\Delta F_{complex}/(1 + K[\text{peptide}])$] or with the entire fluorescence change occurring on binding of the first ligand. We assumed the formation of a 1:1 complex considering the good quality of the fitting obtained using an equation for one binding site and the Scatchard plot. Apparent binding constant values, which were obtained by curve fitting analyses of the titration binding curves, were 1.29 ± 0.16 and 4.15 ± 1.0 μM for the nonacetylated and acetylated peptide, respectively. Both the Scatchard and curve fitting analyses provide nearly identical values for the binding
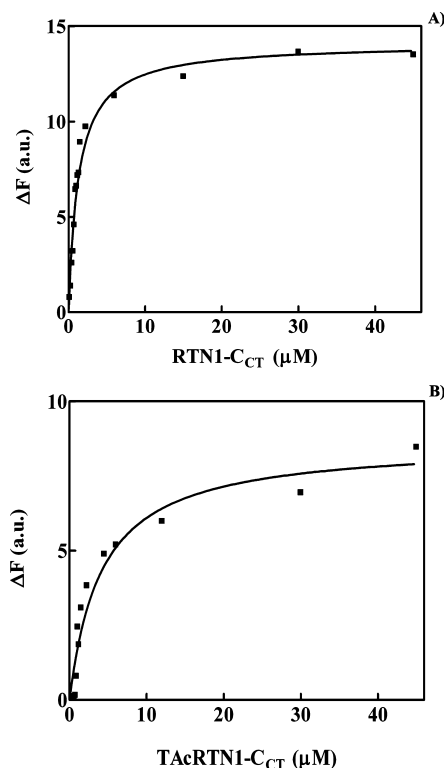

FIGURE 10: Interaction of nonacetylated and fully acetylated forms of RTN1-C_{CT} peptide with HDAC8. Intrinsic fluorescence changes of 1.5 μM HDAC8, in 25 mM Tris-HCl (pH 8.0), 0.1 M NaCl, and 2 mM KCl, with the increase in RTN1-C_{CT} concentration (from 0 to 30 equiv) (A) and TAcRTN1-C_{CT} (B). All the experiments were performed at 27 °C.
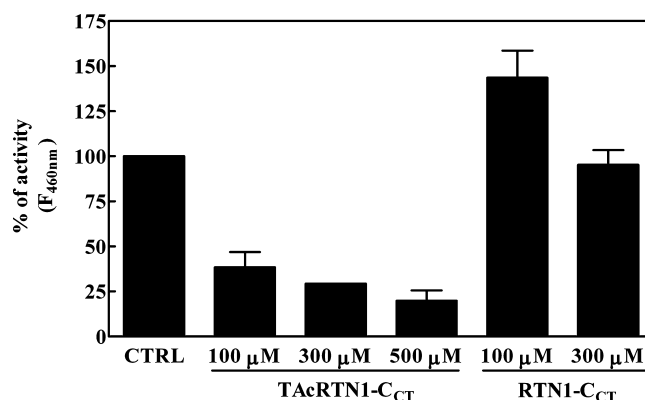

FIGURE 11: Activity profile of HDAC8 in the presence of RTN1-C fragments. HDAC8 (1.12 μM) in 50 mM Tris-HCl (pH 8.0), 137 mM NaCl, 2.7 mM KCl, and 1 mM MgCl$_2$ was preincubated in the presence of different concentrations of TAcRTN1-C_{CT} (100, 300, and 500 μM) or RTN1-C_{CT} (100 and 300 μM) for 15 min at room temperature. The enzyme activity assay was started by substrate addition (see Experimental Procedures).

constants. To evaluate the effect of RTN1-C_{CT} on HDAC8 as an inhibitor, HDAC activity assays of both the acetylated and nonacetylated forms of the peptide were performed. Figure 11 shows the activity profile of HDAC8 in the presence of acetylated and nonacetylated RTN1-C_{CT} peptide. Decreases of 60% and 80% in the HDAC activity were observed when the enzyme was incubated in the presence of 100 and 500 μM TAcRTN1-C_{CT}, respectively. By contrast, an increase of 43% in HDAC8 activity in the presence of RTN1-C_{CT} was observed. The fluorescence values observed

were subtracted from the fluorescence of the acetylated substrate in the presence of the peptide.

While the nonacetylated peptide did not exhibit any inhibitory effect, the fully acetylated peptide exhibited an inhibition of the HDAC activity in a concentration-dependent manner (Figure 11). Approximately 80% of the activity was suppressed when HDAC8 was preincubated for 10 min in the presence of 500 μM TAcRTN1-C$_{CT}$. The inhibition of the HDAC activity may suggest that the enzyme recognizes acetyl groups of TAcRTN1-C$_{CT}$ and that the peptide interaction occurs close the active site of the enzyme. The use of the fluorogenic substrate in the HDAC activity assay was justified by the fact that the fluorophore does not affect the reactivity of the enzyme binding to the enzyme or RTN1-C$_{CT}$, as shown previously by Vannini et al. (*38*) and by our experimental results using the deacetylated Fluor de-Lys (see Figure 8S of the Supporting Information). The deacetylation of TAcRTN1-C$_{CT}$ peptide after reaction with HDAC8 was also investigated by RP-HPLC. No deacetylated forms of the peptide were observed even after reaction for 4 h using 600 μM TAcRTN1-C$_{CT}$ and 2.0 μM HDAC8 at 37 °C (data not shown), suggesting that the peptide was an inactive substrate of the enzyme.

DISCUSSION

The structural homology model of RTN1-C showed that the C-terminal region corresponding to residues 179−208 is external to the membrane and could be located in the cytoplasm (*32, 33*), but the function of this region has not been clarified. Here we biochemically characterize this region for improving our knowledge of the physiological role of this ER protein. The experimental data, reported here, are in agreement with the secondary structure prediction and indicate a good propensity of the RTN1-C$_{CT}$ fragment to assume a helical conformation in a hydrophobic environment. The probable presence of a stable helix conformation, which was predicted to be from residue 190 to 199, could play an important role in the interaction of this protein with other macromolecules.

In the RTN1-C protein, we found a characteristic sequence motif (GAKRH), which is a signature pattern of H4 histone and is an important DNA-binding site of the histone protein. By sequential pattern analysis, we found that RTN1 proteins, together with a spore-specific catalase A, are the only non-histone proteins that have this consensus sequence with 100% identity. On the basis of this observation, we assayed the ability of the RTN1-C$_{CT}$ fragment to bind the nucleic acids. Much experimental evidence, reported here, shows a strong ability of this region to interact with the nucleic acids. A mobility shift assay showed that this fragment was able to bind both DNA and RNA in vitro probably due to the presence of positively charged amino acids and to the H4 consensus sequence. Interestingly, our results, obtained via a fluorescence replacement binding assay, indicated that RTN1-C$_{CT}$ peptide also exhibits an ability to induce a DNA condensation in a time-dependent manner. The reported results of T_m and Eth Br displacement experiments indicate that RTN1-C$_{CT}$ was also able to bind ds[CG], but the affinity for DNA increased with an increase in A·T base pair content. This ability highlights the biological function of the cytosolic C-terminal region of RTN1-C. DNA condensation can

influence gene expression and transcription in vivo; thus, the nucleic acid binding property of the C-terminal region of RTN1-C may be also related to induction of neuronal apoptosis, which recently has been observed in tumor cells after overexpression of RTN1-C protein (*6*). In fact, it is notable that neuronal apoptosis with DNA condensation has been observed in the case of peptides, such as the amyloid β peptide (Aβ) (*39*), which induces time-dependent DNA condensation (*40*). The ability of RTN1-C protein to interact with DNA could be correlated with an important role of the ER membrane. In a recent report, many nuclear envelope (NE) proteins that are dispersed in the ER during mitosis have been shown to possess DNA binding activity (*41*). The nuclear envelope, which compartmentalizes eukaryotic cells into the nucleoplasm and cytoplasm, forms a continuous membrane system with the ER (*42, 43*). In a recent study, the formation of the NE from the intact ER has been recapitulated in vitro; in fact, ER membrane tubules rapidly covered the chromatin surface (*44*). That study also suggested that the intrinsic capacity of the ER to form sheets is utilized and coordinated by chromatin to mediate the rapid conversion of the ER network into NE sheets. Moreover, the study has highlighted a mechanistic role of DNA binding in ER reorganization on chromatin, showing, further, that interactions of the ER with chromatin are mediated by proteins residing in the ER (*44*). On these bases, we propose that the DNA binding ability of RTN1-C protein, here reported, may play a key role in the formation of the NE, although we are aware that further studies are required to confirm this hypothesis.

On the other hand, the involvement of RTNs in cell division was previously hypothesized; in fact, during mitotic cell division, RTNs have been shown to be in a ringlike structure surrounding the spindle apparatus (*45*), and it has been suggested that RTNs might be responsible for the distribution of endomembranes to the two daughter cells during mitotic division.

Our data show that the total acetylation of RTN1-C$_{CT}$ peptide leads to a marked reduction in its ability to bind and condense the DNA; thus, the acetylation−deacetylation process may be a regulator of this function. Recently, we have observed that RTN1-C protein expressed in a human neuroblastoma cell line was acetylated and that this acetylation was dependent on the HDAC activity (M. Piacentini et al., manuscript in preparation). To evaluate if RTN1-C−nucleic acid binding, like that of H4 histone protein, can be regulated in vivo by an acetylation−deacetylation mechanism, the possible interaction of RTN1-C with HDAC enzymes was investigated. More than 40 years ago, modifications such as acetylation were proposed to have functional roles in modulating transcription efficiency (*46*). Acetylation occurs at the ε-amino groups of lysine residues present within the N-terminal extensions of the histones and some non-histone proteins that were found to be transcription factors, heat shock proteins, and structural proteins (*16, 28*). In the past several years, acetylation has been shown to deeply influence either the metabolic stability or the biological function of the modified protein; in fact, with phosphorylation, for example, it is a post-transcriptional mechanism for controlling the protein function. Acetylated proteins can regulate different cellular processes, such as microtubule function or nuclear import (*47, 48*). The balance of HAT

and HDAC enzyme families tightly controls the acetylation status of target lysines (*16, 28*). HDACs catalyze the removal of the acetyl group from the acetyllysine residue, and these enzymes have been divided into four classes according to phylogenetic analyses and sequence homologies (*49, 50*). With the exception of HDAC8, functional HDACs are never found as single monomeric polypeptides; rather, they accumulate in high-molecular weight multiprotein complexes in which different HDAC subtypes are often associated with specific coregulators as well as with other chromatin-modifying enzymes (*51*). We have chosen HDAC8 as a model system for zinc-dependent HDACs and a member of the mammalian class I deacetylases for studying the interaction between RTN1-C$_{CT}$ and HDACs. The binding of HDAC8 to increasing concentrations of RTN1-C$_{CT}$ and TAcRTN1-C$_{CT}$ peptides was assessed by the decrease in the intrinsic fluorescence emission of the enzyme. Eukaryotic HDACs contain a number of tryptophan residues near the active site; in particular, Trp141 is present in the active site of HDAC8, and the fluorescence quenching induced by RTN1-C$_{CT}$ peptide could be due to the interaction of this peptide at the active site. These results indicate the ability of both peptide forms to interact with HDAC8, but the presence of the three other tryptophan residues in the protein and, in particular, the Trp294 residue, which is on the surface of the protein (*38*), does not lead us to establish, with these experiments, unequivocally the site of the interaction. On the other hand, the inhibition of HDAC8 activity by TAcRTN1-C$_{CT}$ could suggest that the interaction is at the active site of the enzyme. However, no deacetylation of TAcRTN1-C$_{CT}$ peptide after reaction with HDAC8 was observed, suggesting that, although the peptide is able to bind and inhibit the enzyme, it is not a good substrate for the enzyme. The acetylation of all Lys residues and of the N-terminus of the peptide leads to a reduction in the positive charge, which could reduce the k_{off} of the final product resulting in HDAC8 inhibition, showing the importance of electrostatic interactions either of the substrate or of the product with the enzyme. Thus, the interaction of different acetylated forms of RTN1-C$_{CT}$ with either HDAC8 or other HDACs remains to be investigated to elucidate this point. Recently, it has been reported that the presence of a KRHR sequence was able to rescue the activity of a local sequence that on its own was a poor substrate (*52*). The activity of HDAC8 for the N-terminal peptide of histone H4 depends on both local and distal sequences of the substrate, even if the native sequence of this histone is not optimized for activity toward this deacetylase (*51*). RTN1-C$_{CT}$ presents a homologous KRHA sequence that may be responsible for the observed trans-activating effect of the nonacetylated peptide, although the R19A substitution in the H4 substrates has been observed to yield a decrease in HDAC activity (*52*). The observed increase in HDAC8 activity in the presence of RTN1-C$_{CT}$ could be explained by the binding of this C-terminal part of the peptide with an exosite of this enzyme. Recently, the presence of an exosite in a distal region from the HDACs active site has been hypothesized. This exosite, like other enzymes (*53−55*), might interact with molecules, or other regions of the peptide substrate, increasing the affinity of the enzyme for its own substrate. In fact, it has been found that resveratrol interacts with SIRT1 at an exosite and can allosterically increase the activity of the enzyme for

its substrate (*56*). Although the presence of an exosite in HDAC8 has not been confirmed, it has been proposed that the substrate specificity derives from interactions of the substrate or separator adaptor proteins with an exosite (*52*). Although fully acetylated RTN1-C$_{CT}$ is an inactive substrate of HDAC8, our data show a possible interaction with it and address a possible interaction with other HDACs. Thus, the function of RTN1-C protein could be regulated in vivo through acetylation, which is similar to the systems in several other proteins which, in their DNA recognition function, stability, or interaction with other molecules, are regulated by this mechanism. A further comparison of the activities of peptide mutants could help, in the future, in precisely identifying the residues involved in the binding to HDAC8. In conclusion, these studies provide initial insights that aid in understanding the physiological role of RTN1-C protein and may represent a relevant starting point for elucidation of the functions of the reticulon family.

SUPPORTING INFORMATION AVAILABLE

pDNA binding of RTN1-C$_{NT(1−32)}$ (Figure 1S), RP-HPLC and PAGE of TAcRTN1-C$_{CT}$ (Figure 2S), LC−MS (ESI) spectrum of TAcRTN1-C$_{CT}$ (Figure 3S), ^{1}H NMR analysis of TAcRTN1-C$_{CT}$ (Figure 4S), secondary structure of TAcRTN1-C$_{CT}$ peptide (CD spectra) (Figure 5S), pDNA binding of TAcRTN1-C$_{CT}$ (Figure 6S), DNA condensation ability of TAcRTN1-C$_{CT}$ (Figure 7S), and fluorescence spectra of DeAcFLys in the presence of RTN1-C$_{CT}$ (Figure 8S). This material is available free of charge via the Internet at http://pubs.acs.org.

REFERENCES

1. Oertle, T., and Schwab, M. E. (2003) Nogo and its paRTNers. *Trends Cell Biol. 13*, 187–194.
2. Roebroek, A. J., van de Velde, H. J., Van Bokhoven, A., Broers, J. L., Ramaekers, F. C., and Van de Ven, W. J. (1993) Cloning and expression of alternative transcripts of a novel neuroendocrine-specific gene and identification of its 135-kDa translational product. *J. Biol. Chem. 268*, 13439–13447.
3. van de Velde, H. J., Senden, N. H., Roskams, T. A., Broers, J. L., Ramaekers, F. C., Roebroek, A. J., and Van de Ven, W. J. (1994) NSP-encoded reticulons are neuroendocrine markers of a novel category in human lung cancer diagnosis. *Cancer Res. 54*, 4769–4776.
4. Dupuis, L., Gonzalez de Aguilar, J. L., di Scala, F., Rene, F., de Tapia, M., Pradat, P. F., Lacomblez, L., Seihlan, D., Prinjha, R., Walsh, F. S., Meininger, V., and Loeffler, J. P. (2002) Nogo provides a molecular marker for diagnosis of amyotrophic lateral sclerosis. *Neurobiol. Dis. 10*, 358–365.
5. Li, S., Liu, B. P., Budel, S., Li, M., Ji, B., Walus, L., Li, W., Jirik, A., Rabacchi, S., Choi, E., Worley, D., Sah, D. W., Pepinsky, B., Lee, D., Relton, J., and Strittmatter, S. M. (2004) Blockade of Nogo-66, myelin-associated glycoprotein, and oligodendrocyte myelin glycoprotein by soluble Nogo-66 receptor promotes axonal sprouting and recovery after spinal injury. *J. Neurosci. 24*, 10511–10520.
6. Di Sano, F., Fazi, B., Tufi, R., Nardacci, R., and Piacentini, M. (2007) Reticulon-1C acts as a molecular switch between endoplasmic reticulum stress and genotoxic cell death pathway in human neuroblastoma cells. *J. Neurochem. 102*, 345–353.

7. Tang, W. F., Yang, S. Y., Wu, B. W., Jheng, J. R., Chen, Y. L., Shih, C. H., Lin, K. H., Lai, H. C., Tang, P., and Horng, J. T. (2007) Reticulon 3 binds the 2C protein of enterovirus 71 and is required for viral replication. *J. Biol. Chem. 282*, 5888–5898.

8. Tagami, S., Eguchi, Y., Kinoshita, M., Takeda, M., and Tsujimoto, Y. (2000) A novel protein, RTN-XS, interacts with both Bcl-XL and Bcl-2 on endoplasmic reticulum and reduces their anti-apoptotic activity. *Oncogene 19*, 5736–5746.

9. Di Sano, F., Fazi, B., Citro, G., Lovat, P. E., Cesareni, G., and Piacentini, M. (2003) Glucosylceramide synthase and its functional interaction with RTN-1C regulate chemotherapeutic-induced apoptosis in neuroepithelioma cells. *Cancer Res. 63*, 3860–3865.

10. Steiner, P., Kulangara, K., Sarria, J. C., Glauser, L., Regazzi, R., and Hirling, H. (2004) Reticulon 1C/neuroendocrine-specific protein-C interacts with SNARE proteins. *J. Neurochem. 89*, 569–580.

11. He, W., Hu, X., Shi, Q., Zhou, X., Lu, Y., Fisher, C., and Yan, R. (2006) Mapping of interaction domains mediating binding between BACE1 and RTN/Nogo proteins. *J. Mol. Biol. 363*, 625–634.

12. Mannan, A. U., Boehm, J., Sauter, S. M., Rauber, A., Byrne, P. C., Neesen, J., and Engel, W. (2006) Spastin, the most commonly mutated protein in hereditary spastic paraplegia interacts with Reticulon 1 an endoplasmic reticulum protein. *Neurogenetics 7*, 93–103.

13. Errico, A., Ballabio, A., and Rugarli, E. I. (2002) Spastin, the protein mutated in autosomal dominant hereditary spastic paraplegia, is involved in microtubule dynamics. *Hum. Mol. Genet. 11*, 153–163.

14. Sanderson, C. M., Connell, J. W., Edwards, T. L., Bright, N. A., Duley, S., Thompson, A., Luzio, J. P., and Reid, E. (2006) Spastin and atlastin, two proteins mutated in autosomal-dominant hereditary spastic paraplegia, are binding partners. *Hum. Mol. Genet. 15*, 307–318.

15. Jahn, R., and Sudhof, T. C. (1999) Membrane fusion and exocytosis. *Annu. Rev. Biochem. 68*, 863–911.

16. Marks, P. A., Miller, T., and Richon, V. M. (2003) Histone deacetylases. *Curr. Opin. Pharmacol. 3*, 344–351.

17. Satz, A. L., and Bruice, T. C. (2001) Recognition of nine base pairs in the minor groove of DNA by a tripyrrole peptide-Hoechst conjugate. *J. Am. Chem. Soc. 123*, 2469–2477.

18. Boger, D. L., Fink, B. E., Brunette, S. R., Tse, W. C., and Hedrick, M. P. (2001) A simple, high-resolution method for establishing DNA binding affinity and sequence selectivity. *J. Am. Chem. Soc. 123*, 5878–5891.

19. Cary, P. D., Crane-Robinson, C., Bradbury, E. M., and Dixon, G. H. (1982) Effect of acetylation on the binding of N-terminal peptides of histone H4 to DNA. *Eur. J. Biochem. 127*, 137–143.

20. Vannini, A., Volpari, C., Filocamo, G., Casavola, E. C., Brunetti, M., Renzoni, D., Chakravarty, P., Paolini, C., De Francesco, R., Gallinari, P., Steinkuhler, C., and Di Marco, S. (2004) Crystal structure of a eukaryotic zinc-dependent histone deacetylase, human HDAC8, complexed with a hydroxamic acid inhibitor. *Proc. Natl. Acad. Sci. U.S.A. 101*, 15064–1509.

21. Combet, C., Blanchet, C., Geourjon, C., and Deleage, G. (2000) NPS@: Network protein sequence analysis. *Trends Biochem. Sci. 25*, 147–150.

22. Ebralidse, K. K., Grachev, S. A., and Mirzabekov, A. D. (1988) A highly basic histone H4 domain bound to the sharply bent region of nucleosomal DNA. *Nature 331*, 365–367.

23. Dorigo, B., Schalch, T., Bystricky, K., and Richmond, T. J. (2003) Chromatin fiber folding: Requirement for the histone H4 N-terminal tail. *J. Mol. Biol. 327*, 85–96.

24. Chiani, F., Di Felice, F., and Camilloni, G. (2006) SIR2 modifies histone H4-K16 acetylation and affects superhelicity in the ARS region of plasmid chromatin in *Saccharomyces cerevisiae*. *Nucleic Acids Res. 34*, 5426–5437.

25. Doenecke, D., and Gallwitz, D. (1982) Acetylation of histones in nucleosomes. *Mol. Cell. Biochem. 44*, 113–128.

26. Shogren-Knaak, M., Ishii, H., Sun, J. M., Pazin, M. J., Davie, J. R., and Peterson, C. L. (2006) Histone H4-K16 acetylation controls chromatin structure and protein interactions. *Science 311*, 844–847.

27. Roth, S. Y., Denu, J. M., and Allis, C. D. (2001) Histone acetyltransferases. *Annu. Rev. Biochem. 70*, 81–120.

28. Di Gennaro, E., Bruzzese, F., Caraglia, M., Abruzzese, A., and Budillon, A. (2004) Acetylation of proteins as novel target for antitumor therapy: Review article. *Amino Acids 26*, 435–441.

29. Andrade, M. A., Chacon, P., Merelo, J. J., and Moran, F. (1993) Evaluation of secondary structure of proteins from UV circular dichroism spectra using an unsupervised learning neural network. *Protein Eng. 6*, 383–390.

30. Aurora, R., and Rose, G. D. (1998) Helix capping. *Protein Sci. 7*, 21–38.

31. Dragani, B., Stenberg, G., Melino, S., Petruzzelli, R., Mannervik, B., and Aceto, A. (1997) The conserved N-capping box in the hydrophobic core of glutathione S-transferase P1-1 is essential for refolding. Identification of a buried and conserved hydrogen bond important for protein stability. *J. Biol. Chem. 272*, 25518–25523.

32. GrandPre, T., Nakamura, F., Vartanian, T., and Strittmatter, S. M. (2000) Identification of the Nogo inhibitor of axon regeneration as a Reticulon protein. *Nature 403*, 439–444.

33. Fazi, B., Melino, S., Di Sano, F., Cicero, D. O., Piacentini, M., and Paci, M. (2006) Cloning, expression, and preliminary structural characterization of RTN-1C. *Biochem. Biophys. Res. Commun. 342*, 881–886.

34. Hsu, C. H., Chen, C., Jou, M. L., Lee, A. Y., Lin, Y. C., Yu, Y. P., Huang, W. T., and Wu, S. H. (2005) Structural and DNA-binding studies on the bovine antimicrobial peptide, indolicidin: Evidence for multiple conformations involved in binding to membranes and DNA. *Nucleic Acids Res. 33*, 4053–4064.

35. Melino, S., Gallo, M., Trotta, E., Mondello, F., Paci, M., and Petruzzelli, R. (2006) Metal-binding and nuclease activity of an antimicrobial peptide analogue of the salivary histatin 5. *Biochemistry 45*, 15373–15383.

36. LePecq, J. B., and Paoletti, C. (1967) A fluorescent complex between ethidium bromide and nucleic acids. Physical-chemical characterization. *J. Mol. Biol. 27*, 87–106.

37. Hong, L., Schroth, G. P., Matthews, H. R., Yau, P., and Bradbury, E. M. (1993) Studies of the DNA binding properties of histone H4 amino terminus. Thermal denaturation studies reveal that acetylation markedly reduces the binding constant of the H4 "tail" to DNA. *J. Biol. Chem. 268*, 305–314.

38. Vannini, A., Volpari, C., Gallinari, P., Jones, P., Mattu, M., Carfi, A., De Francesco, R., Steinkuhler, C., and Di Marco, S. (2007) Substrate binding to histone deacetylases as shown by the crystal structure of the HDAC8-substrate complex. *EMBO Rep. 8*, 879–884.

39. Pillot, T., Drouet, B., Queille, S., Labeur, C., Vandekerchkhove, J., Rosseneu, M., Pincon-Raymond, M., and Chambaz, J. (1999) The nonfibrillar amyloid β-peptide induces apoptotic neuronal cell death: Involvement of its C-terminal fusogenic domain. *J. Neurochem. 73*, 1626–1634.

40. Yu, H., Ren, J., and Qu, X. (2007) Time-dependent DNA condensation induced by amyloid β-peptide. *Biophys. J. 92*, 185–191.

41. Ulbert, S., Platani, M., Boue, S., and Mattaj, I. W. (2006) Direct membrane protein-DNA interactions required early in nuclear envelope assembly. *J. Cell Biol. 173*, 469–476.

42. D'Angelo, M. A., and Hetzer, M. W. (2006) The role of the nuclear envelope in cellular organization. *Cell. Mol. Life Sci. 63*, 316–332.

43. Burke, B., and Ellenberg, J. (2002) Remodelling the walls of the nucleus. *Nat. Rev. Mol. Cell Biol. 3*, 487–497.

44. Anderson, D. J., and Hetzer, M. W. (2007) Nuclear envelope formation by chromatin-mediated reorganization of the endoplasmic reticulum. *Nat. Cell Biol. 9*, 1160–1166.

45. Taketomi, M., Kinoshita, N., Kimura, K., Kitada, M., Noda, T., Asou, H., Nakamura, T., and Ide, C. (2002) Nogo-A expression in mature oligodendrocytes of rat spinal cord in association with specific molecules. *Neurosci. Lett. 332*, 37–40.

46. Allfrey, V. G., Faulkner, R., and Mirsky, A. E. (1964) Acetylation and Methylation of Histones and Their Possible Role in the Regulation of RNA Synthesis. *Proc. Natl. Acad. Sci. U.S.A. 51*, 786–794.

47. Takemura, R., Okabe, S., Umeyama, T., Kanai, Y., Cowan, N. J., and Hirokawa, N. (1992) Increased microtubule stability and α tubulin acetylation in cells transfected with microtubule-associated proteins MAP1B, MAP2 or tau. *J. Cell Sci. 103* (Part 4), 953–964.

48. Bannister, A. J., Miska, E. A., Gorlich, D., and Kouzarides, T. (2000) Acetylation of importin-α nuclear import factors by CBP/p300. *Curr. Biol. 10*, 467–470.

49. de Ruijter, A. J., van Gennip, A. H., Caron, H. N., Kemp, S., and van Kuilenburg, A. B. (2003) Histone deacetylases (HDACs): Characterization of the classical HDAC family. *Biochem. J. 370*, 737–749.

50. Blander, G., and Guarente, L. (2004) The Sir2 family of protein deacetylases. *Annu. Rev. Biochem. 73*, 417–435.

51. Chan, J. K., Sun, L., Yang, X. J., Zhu, G., and Wu, Z. (2003) Functional characterization of an amino-terminal region of HDAC4 that possesses MEF2 binding and transcriptional repressive activity. *J. Biol. Chem. 278*, 23515–23521.

52. Gurard-Levin, Z. A., and Mrksich, M. (2008) The activity of HDAC8 depends on local and distal sequences of its peptide substrates. *Biochemistry 47*, 6242–6250.

53. Overall, C. M. (2001) Matrix metalloproteinase substrate binding domains, modules and exosites. Overview and experimental strategies. *Methods Mol. Biol. 151*, 79–120.

54. Biondi, R. M., and Nebreda, A. R. (2003) Signalling specificity of Ser/Thr protein kinases through docking-site-mediated interactions. *Biochem. J. 372*, 1–13.

55. Krishnaswamy, S. (2005) Exosite-driven substrate specificity and function in coagulation. *J. Thromb. Haemostasis 3*, 54–67.

56. Howitz, K. T., Bitterman, K. J., Cohen, H. Y., Lamming, D. W., Lavu, S., Wood, J. G., Zipkin, R. E., Chung, P., Kisielewski, A., Zhang, L. L., Scherer, B., and Sinclair, D. A. (2003) Small molecule activators of sirtuins extend *Saccharomyces cerevisiae* lifespan. *Nature 425*, 191–196.

57. Thompson, J. D., Higgins, D. G., and Gibson, T. J. (1994) CLUSTAL W: Improving the sensitivity of progressive multiple sequence alignment through sequence weighting, position-specific gap penalties and weight matrix choice. *Nucleic Acids Res. 22*, 4673–4680.

58. Garnier, J., Gibrat, J. F., and Robson, B. (1996) GOR secondary structure prediction method version IV. *Methods Enzymol. 266*, 540–553.